JVI Journals.ASM.org

Role for a Zinc Finger Protein (Zfp111) in Transformation of 208F Rat Fibroblasts by Jaagsiekte Sheep Retrovirus Envelope Protein

Tom Hsu,[a] An Phung,[a] Kevin Choe,[a] Jung Woo Kim,[b] Hung Fan[a]

Department of Molecular Biology and Biochemistry and Cancer Research Institute, University of California, Irvine, Irvine, California, USA[a]; Department of Life Science Technology, Pai Chai University, Seo-gu, Daejeon, South Korea[b]

ABSTRACT

The native envelope gene (*env*) of Jaagsiekte sheep retrovirus (JSRV) also acts as an oncogene. To investigate the mechanism of transformation, we performed yeast 2-hybrid screening for cellular proteins that interact with Env. Among several candidates, we identified mouse or rat zinc finger protein 111 (*zfp111*). The interaction between Env and Zfp111 was confirmed through *in vivo* coimmunoprecipitation assays. Knockdown of endogenous Zfp111 caused a decrease in cell transformation by JSRV Env, while overexpression of Zfp111 increased overall Env transformation, supporting a role for Zfp111 in Env transformation. Knockdown of Zfp111 had no effect on the growth rate of parental rat 208F cells, while it decreased the proliferation rate of JSRV-transformed 208F cells, suggesting that JSRV-transformed cells became dependent on Zfp111. In addition, Zfp111 preferentially bound to a higher-mobility form of JSRV Env that has not been described previously. The higher-mobility form of Env (P70^{env}) was found exclusively in the nuclear fraction, and size of its polypeptide backbone was the same as that of the cytoplasmic Env polyprotein (Pr80^{env}). The differences in glycosylation between the two versions of Env were characterized. These results identify a novel cellular protein, Zfp111, that binds to the JSRV Env protein, and this binding plays a role in Env transformation. These results indicate that JSRV transformation also involves proteins and interactions in the nucleus.

IMPORTANCE

The envelope protein (Env) of Jaagsiekte sheep retrovirus (JSRV) is an oncogene, but its mechanism of cell transformation is still unclear. Here we identified seven candidate cellular proteins that can interact with JSRV Env by yeast two-hybrid screening. This study focused on one of the seven candidates, zinc finger protein 111 (Zfp111). Zfp111 was shown to interact with JSRV Env in cells and to be involved in JSRV transformation. Moreover, coexpression of JSRV Env and Zfp111 led to the identification of a novel nuclear form of the JSRV Env protein that binds Zfp111. Nuclear Env was found to differ by glycosylation from the cytoplasmic Env precursor to the virion envelope proteins. These results suggest that JSRV Env transformation may involve nuclear events such as an alteration in transcription mediated by Env-Zfp111 interactions.

Jaagsiekte sheep retrovirus (JSRV) is a betaretrovirus that causes ovine pulmonary adenocarcinoma (OPA), a contagious lung cancer in sheep that reflects malignant transformation of lung secretory epithelial cells (1, 2). OPA is morphologically similar to human lepidic adenocarcinoma, formerly known as bronchioloalveolar carcinoma (more recently designated adenocarcinoma *in situ* [AIS]) (3), a type of lung cancer that is less associated with cigarette smoke, and it is a good model for this type of human lung cancer (4–6).

JSRV is a simple retrovirus that contains the standard retroviral genes *gag*, *pro*, *pol*, and *env* (7). While JSRV does not carry a transduced cellular oncogene, in experimental inoculation of lambs, it induces tumors rapidly (as early as 10 days), similar to acute transforming retroviruses that carry viral oncogenes (8, 9). Interestingly, the JSRV envelope protein (Env) also functions as an oncogene in that the expression of JSRV Env alone can transform NIH 3T3 mouse (10), 208F rat (11), and DF-1 chicken (12) fibroblasts and MDCK canine epithelial cells (13) and can induce lung cancer in mice (14, 15) and sheep (16). Thus, JSRV Env has the rare feature of acting as both the envelope protein for the virus as well as an oncogene for cell transformation. This feature is shared only by a closely related retrovirus, enzootic nasal tumor virus (ENTV), which causes epithelial tumors in the nasal passages of infected animals (17) and expresses an Env protein that alone can transform NIH 3T3 mouse and 208F rat fibroblasts (18, 19).

JSRV Env is initially translated from spliced viral mRNA into a polyprotein that is a type I transmembrane protein of ~615 amino acids (2, 7, 20). The Env polyprotein is cleaved by cellular furin protease into the surface (SU) and transmembrane (TM) proteins. The SU protein is responsible for receptor binding, and TM is responsible for the fusion of viral and cellular membranes upon infection. TM contains a 45-amino-acid cytoplasmic tail (CT) region that extends into the cytoplasm of the cell. The CT of Env contains the sequence YRNM, a putative binding site for the regulatory subunit (p85) of phosphatidylinositol 3-kinase (PI3K) if the tyrosine residue is phosphorylated (21). Mutations in the YRNM tyrosine residue (Y590F or Y590D) inhibited Env transformation in NIH 3T3 mouse and 208F rat fibroblasts (22–24) and

Received 23 June 2015 **Accepted** 29 July 2015

Accepted manuscript posted online 5 August 2015

Citation Hsu T, Phung A, Choe K, Kim JW, Fan H. 2015. Role for a zinc finger protein (Zfp111) in transformation of 208F rat fibroblasts by Jaagsiekte sheep retrovirus envelope protein. J Virol 89:10453–10466. doi:10.1128/JVI.01631-15.

Editor: K. L. Beemon

Address correspondence to Hung Fan, hyfan@uci.edu.

doi:10.1128/JVI.01631-15

tumorigenesis in sheep (25). However, tyrosine phosphorylation has not been detected in TM in JSRV80-transformed cells (24), pulldown experiments have not demonstrated a direct interaction between JSRV Env and PI3K (26), and inactivating mutations in the YRNM tyrosine residue did not affect the transformation of DF-1 chicken cells (12). Nevertheless, a downstream substrate of PI3K, Akt, is constitutively phosphorylated in JSRV-transformed cells, and PI3K inhibitors revert JSRV-transformed cells back toward the nontransformed phenotype (24, 27, 28). Thus, the CT of TM (and the YRNM motif in particular) is necessary for JSRV transformation, although this may not result directly from binding of PI3K.

The signaling pathways activated by JSRV Env transformation have also been studied. Both the PI3K-Akt-mTOR and Ras–MEK–mitogen-activated protein kinase (MAPK) pathways appear to be important for JSRV transformation, as indicated by the inhibition of transformation by inhibitors of different enzymes in these pathways (22, 24, 27, 29). However, an inhibitor of PI3K-Akt-mTOR signaling, rapamycin, indicated that the relative importance of these pathways for JSRV transformation differs among different cell lines. So far, none of the proteins/enzymes in these signaling pathways have been found to directly interact with JSRV Env. Thus, it will be important to identify cellular proteins that interact with JSRV Env and activate these downstream signaling pathways.

In the experiments described here, a yeast 2-hybrid screen was performed by using both full-length JSRV Env and only the cytoplasmic tail (CT) of JSRV Env as baits to identify candidate cDNAs of cellular proteins that interact with JSRV Env. One candidate protein identified was a mouse zinc finger protein of the Krüppel family, zinc finger protein 111 (Zfp111). Validation of Zfp111 as an Env binding protein involved in transformation is described in this report. In addition, Zfp111 was found to interact with a novel nuclear form of JSRV Env, P70^{env}. Characterization of P70^{env}, including its glycosylation, is also reported here.

MATERIALS AND METHODS

Cell lines. Human embryonic kidney HEK 293T (ATCC CRL-3216) and rat fibroblast 208F (30) cells were grown in Dulbecco's modified Eagle's medium supplemented with 10% fetal bovine serum, penicillin (100 U/ml), and streptomycin (100 μg/ml).

Plasmid constructs. The JSRV Env expression plasmid (ΔGP) and the FLAG-tagged version were previously described (10, 31). The v-*mos* expression plasmid was previously described (32).

The hemagglutinin (HA)-tagged mouse *zfp111* expression vector was generated by PCR amplifying mouse *zfp111* cDNA from Open Biosystems with primers 5′-TCCCCGGTCGACAGAACAATGACCAAGTTA and 5′-TCCCCGGCGGCCGCTTAAGCGTAGTCCGGAACGTCGTACGG GTAATCGGAAGTGTGAGGCCTGAT, which was then cloned into pCMV-SPORT6 (Open Biosystems) using SalI and NotI. The HA-tagged rat *zfp111* expression vector was generated by collecting total RNA from rat 208F cells and converting RNA into cDNA by using a 5′/3′ rapid amplification of cDNA ends (RACE) kit (Roche) according to the manufacturer's instructions. The cDNA was amplified by using primers 5′-CG CGGCCGGTCCTTTCTAG and 5′-CCACACTGCTAACCGTGAGGG, and the PCR product was cloned into the pGEM-T vector (Promega). Rat cDNA was subcloned into pCMV-SPORT6 by using primers 5′-TCCCC GGTCGACAGAACGATGACCAAGTTA and 5′-TCCCCGGCGGC CGCTTAAGCGTAGTCCGGAACGTCGTACGGGTAACCGTG CAGGGTTTTTTCTCC and by using SalI and NotI. Mutant *zfp111* was generated via site-directed mutagenesis at the target site of r36-2 short hairpin RNA (shRNA) and was accomplished with two sets of primers (5′-AGCGCTACTGGTGCCACGA with 5′-TCGTGGCACCAGTAG CGGT and 5′-AGCGATATTGGTGCCACGA with 5′-TCGTGGCACCA ATATCGCT).

Yeast two-hybrid screen. pEG 202 (developed by Gyuris and coworkers [33]) was used as the vector to express the LexA-JSRV Env fusion protein. It contains the *his3* selectable marker, a yeast 2μ origin, an *Escherichia coli* pBR origin, and a LexA DNA binding domain. These plasmids (containing the Env fusions) were used as bait.

A human HeLa cell cDNA library and also a mouse liver cDNA library were constructed in the transcription activator B42 fusion vector pJG4-5 (33). Plasmid pJG4-5 contains the TRP1 selectable marker, a yeast 2μ origin, and an *E. coli* pUC origin. Expression of the fusion protein in this plasmid is under the control of GAL1, a galactose-inducible promoter. For the first screen, yeast strain EGY48/pEGLex-JSRV Env was transformed with the HeLa cell cDNA library by the lithium acetate method. Transformants were selected for tryptophan prototrophy in medium lacking uracil, histidine, and tryptophan and containing 2% glucose. All of the transformants were pooled and respread onto synthetic medium (lacking Ura, His, Trp, and Leu) containing 2% galactose for induction. Cells growing on selection medium were retested on synthetic medium (lacking Ura, His, Trp, and Leu) containing 2% galactose (inducing conditions) and 2% glucose (noninducing conditions) to confirm their growth dependence on galactose. Cells growing only on galactose medium were subjected to further characterization. The selected cells were also streaked onto synthetic medium (lacking Ura, His, and Trp) containing 2% galactose or 2% glucose with 5-bromo-4-chloro-3-indolyl-D-galactoside (X-gal) to test for β-galactosidase activity. The cells expressing both reporter genes only in the presence of galactose were finally chosen for plasmid isolation. The isolated plasmids were transformed into *E. coli* K-12 strain KC8 (*pyrF*::Tn*5 hsdR leuB600 tryC9830 lacD74 strA gslK hisB436*), and transformants containing the recombinant cDNAs were selected by their growth on M9 minimal medium (containing Thi, His, Ura, and Leu and lacking Trp) containing ampicillin. The plasmids were then isolated from Trp-positive (Trp$^+$) *E. coli* transformants and used to confirm the selection results, and cDNA inserts were sequenced *in vitro* by using the B42 primer (5′-CCAGCCTCTTGCTGAGTGGAGATG).

Immunoprecipitation. HEK 293T cells were seeded at 2×10^6 cells in 10-cm dishes overnight and transfected with 14 μg each of mouse Zfp111-HA and ΔGP-FLAG (or pcDNA; 28 μg total) by using the CalPhos mammalian transfection kit (Clontech) according to the manufacturer's instructions. Cells were incubated for 48 h prior to cell lysis. Cells were lysed by sonication in 1% NP-40 lysis buffer (50 mM Tris-HCl [pH 8], 150 mM NaCl, 1% NP-40 substitute, and 1 tablet of Complete Mini EDTA Free [Roche]). Lysates were cleared by centrifugation and precleared by adding 50 μl of protein A-agarose beads (Roche) to the mixture. Supernatants were incubated overnight at 4°C with 2 μl of rabbit anti-HA antibody (Cell Signaling) or with 50 μl of anti-FLAG M2 affinity gel (Sigma). An immunoprecipitation (IP) control was done by adding 2 μl of normal rabbit IgG (Santa Cruz Biotechnology) to the mixture. The next day, 50 μl of protein A-agarose beads was added to samples incubated with rabbit anti-HA antibody or with normal rabbit IgG, and the mixtures were incubated for 4 h. The incubation mixtures were separated into bound (pellet) and unbound (supernatant) fractions by centrifugation in a microcentrifuge for 5 min. After washing of the pellets with lysis buffer, the immunoprecipitated material was eluted from the washed pellets by boiling in 2× Laemmli buffer. Proteins were resolved on 10% SDS-polyacrylamide gels and probed with rabbit anti-FLAG or mouse anti-HA primary antibodies (Cell Signaling) and goat anti-rabbit horseradish peroxidase (HRP) or goat anti-mouse HRP secondary antibodies (Pierce), respectively. Blots were visualized by chemiluminescence with SuperSignal Femto maximum-sensitivity substrate (Pierce).

Zfp111 knockdown and transformation. Construction of the lentiviral shRNA vectors was based on the LVTHm vectors (34). The sense sequences for the shRNAs used here are as follows: 5′-ACACTGTCTGC AGACTCTG for r27-1, 5′-AGCGCTACTGGTGTCATGA for r36-2, and

5′-CCTAAGGTTAAGTCGCCCT for the scrambled control. Vector stocks were generated by transiently transfecting the vector plasmids along with pCMV-dR.8.74 (HIV *gag-pol*) and pMD2G (vesicular stomatitis virus [VSV] G protein) helper plasmids into HEK 293T cells, and supernatants were collected after 48 h. The titers of the lentiviral vector stocks were determined by infection of 208F cells, followed by counting of foci of enhanced green fluorescent protein (EGFP) fluorescence (encoded by the LVTHm vector) after 4 days. For transduction with lentiviral vectors, rat fibroblast 208F cells were seeded into 6-well plates at 3×10^5 cells per well, and the following day, the cells were incubated with vector stocks at multiplicities of infection of 10 or greater in the presence of Polybrene (final concentration, 8 μg/ml) for 24 h. The transduced cells were then trypsinized and seeded for transformation assays.

Transformation assays with transduced 208F cells were performed as follows: 208F cells were seeded at 3×10^5 cells in 6-cm dishes and transfected with 5 μg of ΔGP by using Fugene 6 transfection reagent (Promega). In the transformation restoration assay, transduced 208F cells were cotransfected with 5 μg each of ΔGP and either the wild-type (WT) rat *zfp111* or mutant shRNA-resistant rat *zfp111* expression vector. Cells were examined by phase-contrast microscopy at 4 to 5 weeks, and the number of transformed foci was counted. The numbers of foci relative to those in LVTHm (empty vector)-transduced cells in the same experiment were calculated, and the results from at least three independent experiments were averaged. Statistical analyses for all transformation assays were performed by using Welch's *t* test.

Zfp111 overexpression and transformation. 208F cells were seeded at 3×10^5 cells in 6-cm dishes and transfected by using Fugene 6 with 5 μg ΔGP and up to 5 μg of the mouse *zfp111* expression vector; pcDNA was added to make the total amount of DNA 10 μg. Cells were scored for foci at 4 to 5 weeks as described above.

Quantitative PCR. Total RNA was isolated from cells by using TRIzol reagent (Life Technologies), and 2 μg of RNA was digested with DNase I and converted to cDNA by using a qScript cDNA synthesis kit (Quantas) according to the manufacturer's instructions. The resulting cDNAs were diluted to a final concentration of 20 ng/μl. Primers for the amplification of target genes are as follows: 5′-GAAGCCATTCAAATGCAATGCATGCCA and 5′-CTCTGATGGATTTGAAGACTGGACC for rat *zfp111*, 5′-GAAGCCATTCAAATGCAATGCATGCCA and 5′-GGAGACCAGACCTCTGGCCAAAGG for mouse/rat *zfp111*, and 5′-CACCAGTTCGCCATGGATGACGAT and 5′-TCTCTTGCTCTGGGCCTCGTCG for the rat β-actin housekeeping gene. Quantitative reverse transcriptase PCRs (qRT-PCRs) were performed by using Power SYBR green PCR master mix with the 7900HT Fast real-time PCR system (Applied Biosystems) according to the manufacturer's instructions. All qRT-PCRs were run in triplicate. The RNA expression levels were determined by both absolute standard curve and relative comparative threshold cycle (C_T) methods: normalization of Zfp111 to the housekeeping gene β-actin was done by subtracting the average C_T value of Zfp111 from that its β-actin control, and the C_T change was then calculated by subtracting the C_T of the normalized sample from the C_T of the normalized LVTHm sample.

Cell proliferation assays. 208F cells (parental or Env transformed) transduced with control or *zfp111* shRNA knockdown vectors were seeded at 2.5×10^4 cells in 6-cm dishes. The cells were removed from replicate dishes daily by trypsinization, and the number of cells was determined by counting in a hemacytometer, using trypan blue exclusion to score only live cells.

Subcellular fractionation. HEK 293T cells were plated at 2×10^6 cells in a 10-cm dish. The cells were then transfected with 14 μg each of mouse Zfp111-HA and ΔGP-FLAG (or pcDNA; 28 μg total) by using a CalPhos mammalian transfection kit (Clontech) according to the manufacturer's instructions. Cells were incubated for 48 h prior to cell lysis. Cells were collected by directly washing the cells off the plate using a cold 1× phosphate-buffered saline (PBS) solution. One half of the Env-transfected cells were lysed directly with radioimmunoprecipitation assay (RIPA)-SDS lysis buffer (50 mM Tris-HCl, 150 mM NaCl, 1% NP-40, and 0.5% sodium deoxycholate with 1 tablet of Complete Mini EDTA Free protease inhibitor [Roche]) to be used as the total cell lysate fraction. The other half was harvested by centrifugation at 300 × *g* for 5 min in a 15-ml conical tube, and the cells in the pellet were swelled by incubation in 215 μl hypotonic buffer (10 mM HEPES [pH 7.9 at 4°C], 1.5 mM $MgCl_2$, 10 mM NaCl) for 10 min at 4°C. The cells were lysed by ~50 strokes in a glass Dounce homogenizer with a type B pestle; lysis was monitored by phase-contrast microscopy. The lysate was centrifuged in a 15-ml conical tube at 300 × *g* for 5 min at 4°C, and the supernatant was taken as the cytoplasmic fraction. The remaining pellet was washed by resuspension in hypotonic buffer and then centrifuged as described above; the supernatant was removed; and the pellet was designated the nuclear fraction. The nuclear pellet was resuspended in ionic and nonionic detergent buffer, solution A (a mixture of 1 part 10% sodium deoxycholate with 2 parts 10% Tween 40). Solution A was added at a ratio of 3:17 to the remaining pellet resuspended in hypotonic buffer. After brief mixing by vortexing, nuclei were repelleted by centrifugation at 300 × *g* for 5 min at 4°C, and the supernatant was collected and designated the perinuclear fraction. A total of 215 μl RIPA-SDS lysis buffer was added to the remaining pellet, which was then sonicated by using a 200-W sonifier (Branson) at 25% power for 5 s. One volume of 2× Laemmli buffer was added to all fractions prior to heating (100°C for 5 min). Ten percent of the total volume from each of the fractions was loaded onto a 10% SDS-polyacrylamide slab gel for electrophoresis; after wet transfer to polyvinylidene difluoride (PVDF) membranes (Bio-Rad), blots were probed or reprobed with primary antibodies to mouse anti-HA, rabbit anti-FLAG, rabbit anti-β-tubulin, or rabbit anti-lamin A/C antibodies (Cell Signaling Technologies), followed by probing with secondary antibodies (goat anti-mouse HRP and goat anti-rabbit HRP [Pierce], respectively). The blot was visualized by chemiluminescence (SuperSignal West Femto maximum-sensitivity substrate; Pierce).

Endoglycosidase F and chymotrypsin treatment. HEK 293T cells were plated at 2×10^6 cells in a 10-cm dish. The cells were then transfected with 14 μg each of mouse Zfp111-HA and ΔGP-FLAG (28 μg total) by using a CalPhos mammalian transfection kit (Clontech) according to the manufacturer's instruction. Cells were incubated for 48 h prior to cell lysis. Cells were collected by directly washing the cells off the plate using a cold PBS solution. Total cell lysates in RIPA-SDS lysis buffer were prepared from one half of the transfected HEK 293T cells. The remaining half was incubated with 200 μl 0.5% NP-40 lysis buffer and then centrifuged at 300 × *g* at 4°C for 5 min, and the supernatant was collected as the cytoplasmic fraction. A total of 200 μl RIPA-SDS lysis buffer was added to the remaining nuclear pellet, followed by sonication as described above, to give the nuclear fraction. Protein concentrations of each sample were determined by a Bradford assay (Bio-Rad), and up to 20 μg of protein from each fraction was digested with endoglycosidase F (Endo F) according to the manufacturer's directions (New England BioLabs). For chymotrypsin digestion, the native or deglycosylated proteins were digested with 0.2 to 0.5 μg of chymotrypsin (Promega) in a 20-μl total volume for 1 h at room temperature. The entire digests were loaded onto 10% or 15% SDS-polyacrylamide gels, followed by Western blotting and probing with primary antibody (rabbit anti-FLAG) followed by goat anti-rabbit HRP secondary antibody and visualization by chemiluminescence, as described above. Colored PageRuler prestained protein ladder molecular weight protein markers (Fermentas) were run in parallel on the same gels. Western blots were deprobed by incubating the membrane in deprobe buffer (62.5 mM Tris-HCl [pH 6.7], 2% SDS, 0.7% β-mercaptoethanol) for 30 min at 55°C, and the buffer was replaced with fresh deprobe buffer and then incubated for another 30 min. Afterwards, the membrane was washed four times with 1× Tris-buffered saline–Tween (TBST) and blocked in 5% nonfat skim milk in TBST.

Characterization of JSRV Env glycosylation. Samples from cells transfected with ΔGP-FLAG (or cotransfected with mouse Zfp111-HA) were subjected to partial chymotryptic cleavage and then SDS-PAGE and Western blotting for FLAG, as described above. Chymotryptic fragment

TABLE 1 Candidate JSRV Env-interacting proteins from yeast 2-hybrid screens

Candidate	Bait[a]	Library used[b]	Interaction strength[c]	No. of clones[d]	Normal cell function(s)	Transformation[e]
IKAP	CT	Human	++	1	Component of transcription elongation complex	?
RRM2	CT	Human	++	4	Ribonucleotide reductase regulatory subunit	+
Pontin 52	CT	Human	+	1	Beta-catenin-interacting protein (nuclear); chromatin remodeling; c-*myc* interactor	+
Reptin 52	CT	Human	+	1	Beta-catenin-interacting protein (nuclear); chromatin remodeling; c-*myc* interactor	+
Nm23-H2/NDPK-B	CT	Human	++	1	Nucleoside diphosphate kinase; suppressor or metastasis; transcriptional activator	+
Ferritin	CT	Human	++	1	Fe binding protein	−
Zfp111	Whole Env	Mouse	++	4	Zinc finger protein 111; transcriptional suppressor	?

[a] Two different bait proteins in the screens were used, either the JSRV Env cytoplasmic tail only (CT) or the whole JSRV Env protein.
[b] cDNA libraries from human (HeLa) and mouse (NIH 3T3) cells were screened.
[c] Interaction strengths were based on the relative blue color of colonies on X-gal plates. + and ++ represent the relative interaction strengths, with ++ stronger than +.
[d] Number of independent clones of the same cDNA that were isolated from the screens.
[e] From previous studies reporting a role in cell transformation or tumorigenesis. +, plays a role in transformation in other systems; −, has not been reported to be involved in transformation; ?, uncertain if involved in transformation.

sizes were determined by first measuring the migration distance for each of the molecular mass markers on each gel, which was then used to generate a semilog graph for that blot. This semilog graph was then used to estimate the sizes of the chymotryptic fragment based on their migration. Since the FLAG epitope was at the C terminus of the Env protein, the sizes of the chymotryptic fragments could be used to estimate the sites of chymotryptic cleavage relative to the C terminus. The size differences between each fragment were deduced and normalized to the known sizes of the JSRV Env, SU, and TM regions. To measure the amount of glycosylation between each chymotryptic site, $P70^{env}$ or $Pr80^{env}$ was first treated with Endo F for deglycosylation, followed by partial chymotryptic cleavage to generate deglycosylated chymotryptic fragments. The estimated size of the deglycosylated chymotryptic fragment was subtracted from the estimated size of its corresponding glycosylated chymotryptic fragment. The values shown were the means of values from 4 independent experiments. The N-glycosylation sites on JSRV Env were predicted by using the NetNGlyc 1.0 server prediction program.

RESULTS

Yeast 2-hybrid system screening for cellular proteins that interact with JSRV Env. To identify candidate cellular proteins that interact with JSRV Env, two yeast 2-hybrid screens were performed with bait plasmids containing either the cytoplasmic tail (CT) of Env or full-length JSRV Env, as described in Materials and Methods. In one screen, the bait plasmid was the JSRV Env CT fused to the LexA DNA binding domain, which was stably transfected into cells along with a *his3* gene driven by a promoter with LexA binding sites. They were then transformed with plasmids from a cDNA library from human HeLa cells; the cDNAs were fused to the activation domain of B42. Colonies with candidate interacting proteins were identified by growth on medium selective for His expression. In the second screen, the bait plasmid consisted of the entire JSRV Env protein, and the cDNA library was obtained from mouse liver. The candidate interactor proteins are shown in Table 1. Two candidates were of particular interest based on the strength of the interactions with the bait and isolation of multiple interacting cDNA clones, *RRM2* and *zfp111*. These candidates correspond to the ribonucleotide reductase regulatory subunit and a zinc finger protein with putative transcriptional repressor activity (35), respectively. Studies on the potential role of RRM2 in JSRV transformation will be reported elsewhere. Currently, there are few reports regarding *zfp111* function, especially in the area of cancer. It has been shown that *zfp111* contains 19 zinc finger domains as well as a Krüppel-associated box (KRAB) domain, which suggests function as a transcriptional repressor, and it is highly expressed in neuronal tissue (but expressed at a low level in many other tissues) (35). While Zfp111 was identified as a candidate interacting partner in the screen with the full-length JSRV Env protein, interaction of the *zfp111* cDNAs was also found in a subsequent yeast 2-hybrid assay where the bait plasmid contained only the CT domain (not shown). Thus, the putative area of Zfp111 interaction is located in the cytoplasmic tail of the Env TM protein, which is also the crucial domain for Env-induced cell transformation.

Interaction between Zfp111 and JSRV Env in cells. To examine the interaction between Zfp111 and JSRV Env in mammalian cells, an HA epitope-tagged *zfp111* expression vector was cotransfected along with a FLAG epitope-tagged JSRV Env expression vector (ΔGP-FLAG, which is a JSRV Env expression vector that has a FLAG epitope tag attached to the C terminus of JSRV Env) into HEK 293T cells, and the total cell lysate was incubated with either anti-FLAG or anti-HA antibody-conjugated agarose beads for coimmunoprecipitation. In Fig. 1 (left, middle three lanes), lysates from HEK 293T cells cotransfected with ΔGP-FLAG and Zfp111-HA and then immunoprecipitated with anti-FLAG showed that anti-FLAG was able to successfully pull down JSRV Env and also coimmunoprecipitate Zfp111-HA (eluate lane), demonstrating an interaction between Zfp111 and JSRV Env *in vivo*. The control samples, which included transfection of Zfp111-HA only (Fig. 1, left three lanes) and cotransfection of ΔGP-FLAG and Zfp111-HA but immunoprecipitation with normal rabbit IgG (right three lanes), did not show coprecipitation between the two proteins. (Note that for all immunoprecipitations in Fig. 1, 20 times more eluate was loaded than for the total cell lysate and flowthrough.) As shown in Fig. 1 (right), the reciprocal coimmunoprecipitation using anti-HA was also successful in immunoprecipitating Zfp111-HA and coprecipitating JSRV Env in the samples that were transfected with both expression vectors. Control cells transfected with ΔGP-FLAG showed no coprecipitation of Env. Doubly transfected cell lysates immunoprecipitated with only normal rabbit IgG also showed some Env in the eluate, but it was less than that when the lysates were immunopre-

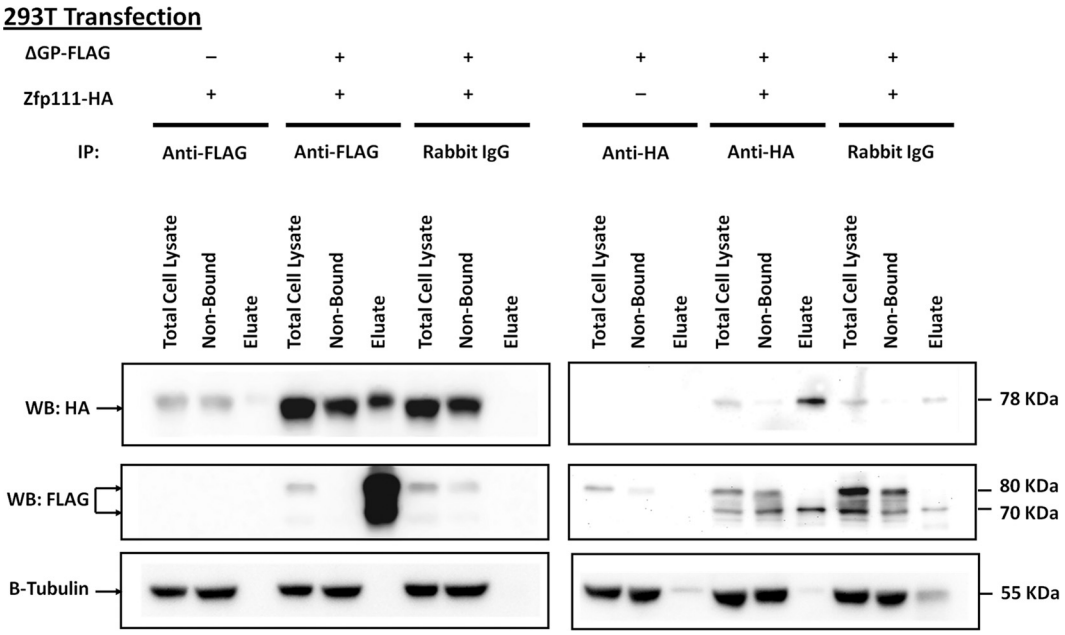

FIG 1 Coimmunoprecipitation of JSRV Env and Zfp111. HEK 293T cells were transfected with ΔGP-FLAG (JSRV Env expression vector with a C-terminal FLAG tag) and mouse Zfp111-HA or pcDNA (−). Total cell lysates were incubated with either anti-HA antibody followed by protein A-Sepharose beads or anti-FLAG affinity gel (purified monoclonal antibody attached to agarose), as described in Materials and Methods. For each lane, equal fractions of the total cell lysate and nonbound fraction and 20 times more eluate were loaded onto a 10% acrylamide gel and analyzed by Western blotting (WB) with either anti-FLAG or anti-HA antibody. Afterwards, the blots were stripped and reprobed with the alternate antibody.

cipitated for Zfp111. In fact, two bands of JSRV Env were observed in lysates from cells transfected with both JSRV Env and Zfp111, and only the lower (more rapidly migrating) band of Env was coprecipitated with Zfp111. This lower band is discussed below. Thus, coimmunoprecipitation of JSRV Env and Zfp111 was observed in transfected HEK 293T cells, suggesting an *in vivo* interaction between the two proteins.

Effects of *zfp111* knockdown and restoration on JSRV Env transformation. To investigate the potential role of Zfp111 in JSRV Env transformation, lentiviral shRNA vectors containing shRNA sequences targeting different areas of rat *zfp111* mRNA were constructed. Lentiviral transduction was chosen since long-term knockdown of *zfp111* was needed during the course of *in vitro* transformation assays (4 to 5 weeks). The control lentiviral vectors (LVTHm and LVTHm-Scrambled) and the shRNA knockdown lentiviral vectors (r27-1 and r36-2) were used to infect rat 208F fibroblasts. The endogenous *zfp111* RNA expression levels were analyzed by qRT-PCR, and normalized expression levels relative to those of infection with LVTHm are shown in Fig. 2A. The most effective *zfp111* shRNA vector, r36-2, showed a decrease in *zfp111* expression levels of 60%, while the r27-1 shRNA vector was less effective. Two more shRNA vectors were tested for *zfp111* knockdown efficiency, but they were not effective in decreasing *zfp111* expression levels (data not shown).

208F cells stably transduced with the vectors shown in Fig. 2A were transfected with the JSRV Env expression vector ΔGP and incubated in focus formation assays (23); the levels of cell transformation were quantified by counting the number of resulting transformed foci for each cell line. For each experiment, the transfections were performed in triplicate, and the experiments were repeated at least three times. The results from a representative experiment are shown in Table 2, and Fig. 2B shows the averaged results, expressed as relative efficiencies of transformation relative to that for cells transduced with the empty shRNA vector LVTHm. For cells transduced with r36-2, there was a statistically significant 40% decrease in JSRV Env transformation compared to that in cells transduced with the control LVTHm and LVTHm-Scrambled vectors (Fig. 2B). Cells transduced with r27-1, which showed less knockdown of *zfp111* expression, did not show a significant decrease in JSRV Env transformation. Knockdown of *zfp111* resulted in a dose-dependent reduction in JSRV Env transformation, consistent with a role of this protein in transformation.

To test if the reduction in JSRV Env transformation by *zfp111* knockdown was specific, the transduced cell lines were also tested in transformation assays with v-*mos*, an oncogene that does not activate the same signaling pathways as those for JSRV Env (29). As also shown in Fig. 2B and Table 2, *zfp111* knockdown had no effect on v-*mos* transformation, particularly in r36-2-transduced cells, where the levels of transformation were similar to those for the LVTHm-transduced cells.

To test if the reduction in JSRV transformation in r36-2-transduced 208F cells was due to knockdown of *zfp111* as opposed to an off-target effect, we tested if restoration of *zfp111* expression in these cells increased JSRV transformation. 208F cells transduced with r36-2 were cotransfected with a rat *zfp111* expression vector containing silent mutations in the r36-2 shRNA recognition site along with the JSRV Env expression vector ΔGP and incubated in focus formation assay mixtures. Quantitative PCR results showed an increase in *zfp111* expression levels compared to those in r36-2-transduced 208F cells (data not shown). As a control, a wild-type (WT) rat *zfp111* expression vector was cotransfected with JSRV Env into the transduced cells. As shown in Fig. 3, r36-2-transduced cells cotransfected with WT *zfp111* showed similar levels of Env transformation as those shown in Fig. 2B, with a 50%

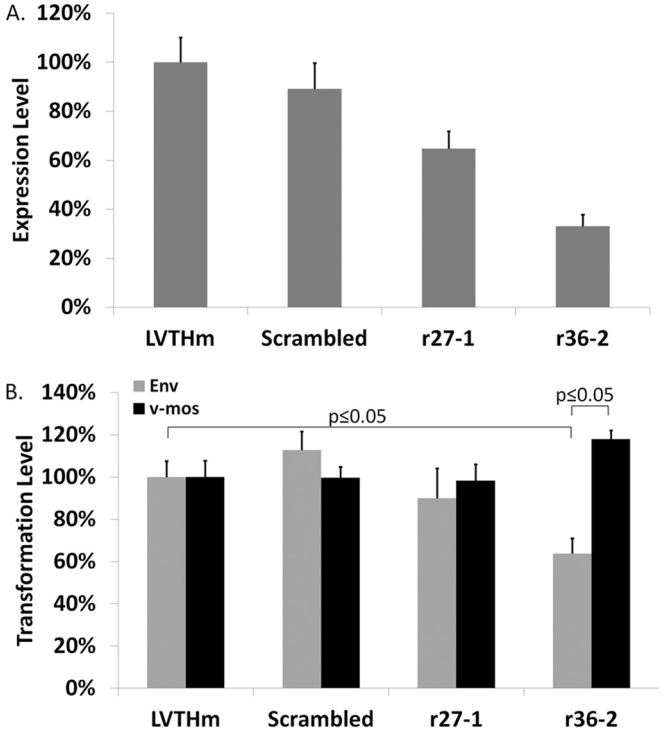

FIG 2 Effects of Zfp111 knockdown on JSRV Env transformation. 208F cells were transduced with the control shRNA vector LVTHm (empty vector) and LVTHm containing a scrambled shRNA (Scrambled-LVTHm) or with r27-1 and r36-2 (shRNAs targeting Zfp111). (A) Zfp111 expression levels in transduced cells were determined by qRT-PCR analysis at 4 to 5 weeks postransduction. (B) Mass cultures of 208F cells recently transduced by each of the vectors were transfected in triplicate with ΔGP DNA and incubated in transformation assay mixtures, and the transformation levels were determined by counting the number of transformed foci at 4 to 5 weeks posttransfection. (Mass cultures were used to minimize the effects of clonal cell variation in response to ΔGP transformation.) The levels of transformation for each shRNA vector were normalized to that for control LVTHm-transduced cells (light gray bars). The means and standard deviations were determined in at least three independent assays; the reduction of JSRV Env transformation in r36-2-transduced cells was statistically significant ($P \leq 0.05$). The same transduced cell cultures were transformed with the v-*mos* oncogene, and transformation assays were performed under the same conditions (black bars). Focus counts from a representative assay are shown in Table 2.

TABLE 2 Effects of Zfp111 knockdown on rat 208F transformation by JSRV Env or v-*mos*[a]

Oncogene cell line	No. of foci		
	Transfection 1	Transfection 2	Transfection 3
ΔGP			
LVTHm	48	51	51
Scrambled	62	61	50
r27-1	51	43	43
r36-2	35	27	29
v-*mos*			
LVTHm	31	31	26
Scrambled	29	31	33
r27-1	29	33	32
r36-2	36	37	34

[a] 208F cells transduced with different lentivirus-based shRNAs were transfected in triplicate with 5 μg of the indicated oncogene plasmid, as described in Materials and Methods. Two shRNA vectors targeted at rat Zfp111 (r27-1 and r36-2) were used. Control vectors included the empty vector (LVTHm) and a vector containing a scrambled shRNA sequence. Parental 208F cells transfected with pcDNA uniformly showed no foci. The cells were incubated for 4 to 5 weeks under focus formation conditions, after which the number of transformed foci was scored. The results from a representative experiment are shown with the focus counts for each of the replicate transfections.

decrease in transformation compared to that of control LVTHm-transduced cells. When the same cells were cotransfected with the mutant *zfp111* plasmid and ΔGP, there was a 30% increase in transformation. In fact, the relative level of transformation (80%), while lower, was not statistically different from that observed for cells transduced with the control LVTHm vector (no *zfp111* knockdown). In cells transduced with the r27-1 knockdown vector, cotransfection with the mutant *zfp111* vector did not enhance JSRV Env transformation (Fig. 3). This was consistent with the fact that the mutant *zfp111* expression plasmid contained the mutated shRNA recognition site for 36-2 but not 27-1 shRNA. This indicated a specificity of the restoration of transformation for the 36-2 knockdown cells and further supported the role of Zfp111 in JSRV transformation.

Effects of *zfp111* overexpression on JSRV Env transformation. In light of the reduction in JSRV Env transformation after *zfp111* knockdown, the effect of *zfp111* overexpression on JSRV Env transformation was also analyzed. 208F cells were cotransfected with different amounts of the *zfp111* expression vector and constant amounts of the JSRV Env expression vector ΔGP. The transfected cells were tested for the levels of *zfp111* RNA expression by qRT-PCR at 4 to 5 weeks posttransfection, at the time when focus formation assays were scored. As shown in Fig. 4A, increasing amounts of the *zfp111* expression vector showed corresponding increases in *zfp111* expression levels. The level of *zfp111* expression in cells treated with 5 μg Zfp111 only was similar to that in cells treated with 5 μg Zfp111 plus 5 μg Env, indicating that Env expression does not increase *zfp111* RNA expression. The transfected cells were plated for transformation assays, and the results are shown in Fig. 4B. Zfp111 alone was not sufficient to induce cell transformation. However, when Zfp111 was cotransfected with JSRV Env, the overall cell transformation levels were higher than those with JSRV Env alone. Furthermore, increasing amounts of Zfp111 showed a dose-dependent increase in transformation levels, with the greatest effect (ca. 2-fold enhancement) being seen for the highest level of Zfp111 (5 μg). To test if this increase in transformation was specific to JSRV Env, these

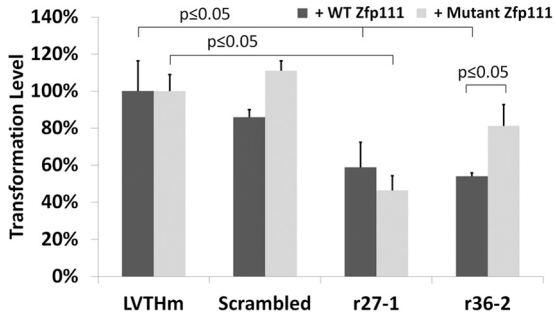

FIG 3 Rescue of transformation by shRNA-resistant Zfp111. Transduced cell cultures similar to those described in the legend of Fig. 2 were transfected with 5 μg ΔGP DNA plus 5 μg of plasmids expressing either WT rat Zfp111 or an r36-2 shRNA-resistant (mutant) rat Zfp111 cDNA. Transformation assays were performed and analyzed as described in the legend of Fig. 2.

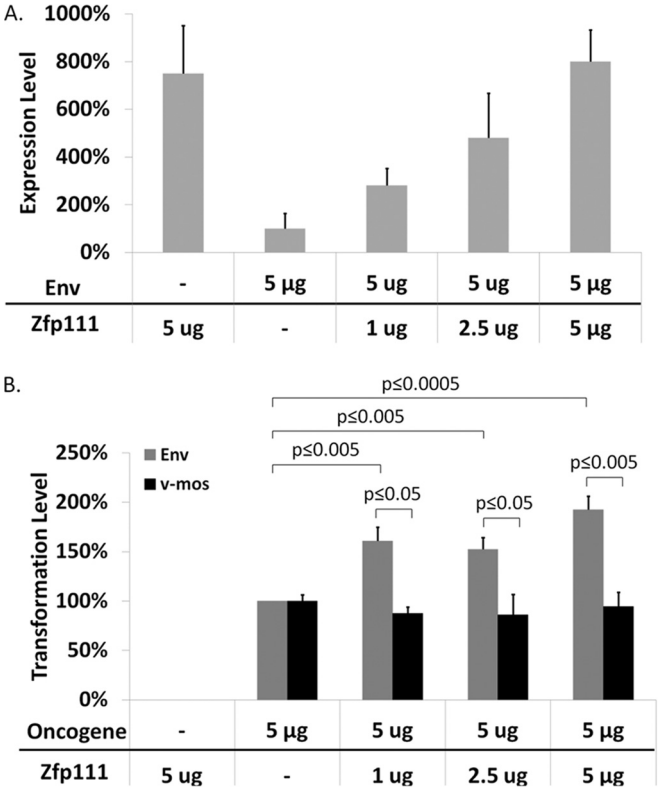

FIG 4 Effects of Zfp111 overexpression on JSRV Env transformation. Rat 208F cells were transfected with ΔGP and/or the WT mouse *zfp111* expression vector, as indicated. A total of 10 μg of plasmid was transfected into each culture, with pcDNA making up the remainder where applicable. (A) Zfp111 expression levels in transfected cells were determined by quantitative RT-PCR analysis. Levels were normalized to values with Env (5 μg) alone. (B) Transfected cultures were incubated in transformation assay mixtures, and transformation levels were determined by counting the numbers of foci. The means and standard deviations were determined from at least two independent assays done in triplicate, and levels were normalized to levels with Env (5 μg) alone (gray bars). Equivalent cultures were cotransfected with the v-*mos* expression vector and different levels of the Zfp111 expression vector, and the results are shown (black bars).

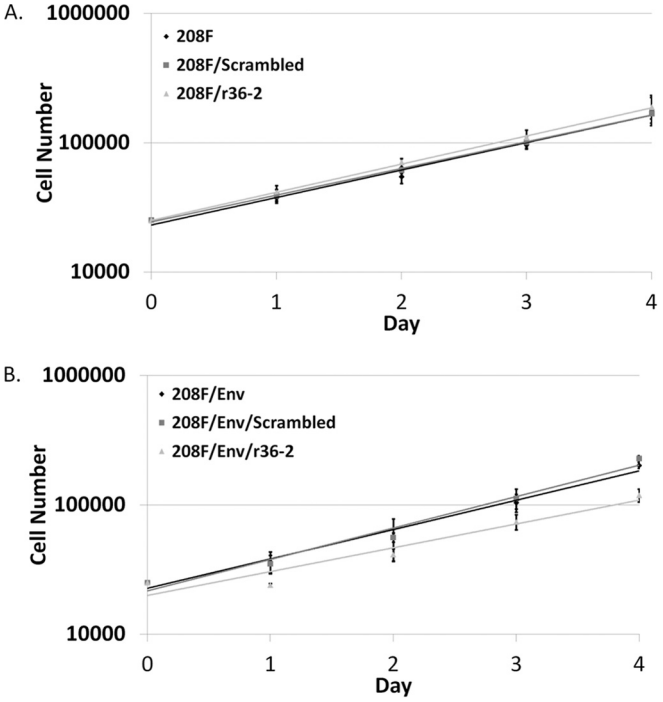

FIG 5 Effects of *zfp111* knockdown on cell proliferation. Untransformed or Env-transformed 208F cells were transduced with scrambled shRNA or *zfp111*-targeting shRNA vectors (scrambled and r36-2, respectively). A total of 2.5×10^4 cells were seeded into wells of 6-well plates, and the number of viable cells was determined by trypsinization and counting of viable cells as measured by trypan blue exclusion over a period of 4 days. The results (semilog plots) from averages of data from three independent experiments, each performed in duplicate, are shown. (A) Growth rates of parental 208F cells and 208F cells transduced with scrambled shRNA and r36-2. (B) Growth rates of JSRV Env-transformed 208F cells and Env-transformed 208F cells transduced with scrambled shRNA and r36-2. The levels of Env expression for these three cell populations were similar, as determined by qRT-PCR (not shown).

cells were also cotransfected with v-*mos* and *zfp111*. As also shown in Fig. 4B, overexpression of zfp111 had no effect on v-*mos* transformation levels, indicating that the Zfp111-mediated increase in transformation was specific to JSRV Env.

Effects of *zfp111* knockdown on cell proliferation. To test if knockdown of *zfp111* affected cell proliferation rates (which could influence focus formation assays), growth rates of three cell lines were measured: untransformed parental 208F cells, 208F cells transduced with the scrambled shRNA vector, and 208F cells transduced with the r36-2 *zfp111* shRNA vector. In Fig. 5A, the proliferation rates for these three cell lines were compared over 4 days, and their growth rates were comparable, as evident from the similar slopes in the semilog plot. This suggested that knockdown of *zfp111* does not affect the growth rates of 208F cells. In Fig. 5B, JSRV Env-transformed 208F cells were transduced with the same two vectors, and the proliferation rates of the resulting cell lines were also measured. Transformed 208F cells and those transduced with the control vector (208F/Env and 208F/Env/Scrambled) showed similar proliferation rates, while transformed cells transduced with the *zfp111* shRNA (208F/Env/r36-2) showed decreased proliferation. Thus, in JSRV Env-transformed cells, knockdown of *zfp111* resulted in a decreased growth rate, suggesting that the growth of JSRV-transformed cells is influenced by Zfp111.

A faster-migrating form of JSRV Env is observed in HEK 293T cells cotransfected with JSRV Env and Zfp111. As shown in Fig. 1, cotransfection of JSRV Env ΔGP and Zfp111 expression vectors into HEK 293T cells led to the appearance of a faster-migrating form of Env. Based on its electrophoretic mobility, this form of JSRV Env (designated $P70^{env}$) was estimated to have a molecular mass of ~70 kDa, lower than that of the standard $Pr80^{env}$ polyprotein (~80 kDa). In addition, $P70^{env}$ was preferentially coimmunoprecipitated with Zfp111, suggesting that it is this form of JSRV Env that interacts with Zfp111. To characterize this form of JSRV Env, HEK 293T cells were transfected with epitope-tagged Zfp111-HA alone, epitope-tagged JSRV Env alone (ΔGP-FLAG), or both. The transfected cells were lysed and also subjected to cell fractionation to determine the intracellular localization of $P70^{env}$. Since $P70^{env}$ was able to bind Zfp111, which is a nuclear protein, it seemed possible that this form of Env may be localized in the nucleus. Western blotting of fractionated cell lysates from cells cotransfected with ΔGP-FLAG and Zfp111-HA showed that $P70^{env}$ was found in the total cell lysate at lower levels than $Pr80^{env}$, and it was enriched in the nuclear fraction (Fig. 6A). Moreover,

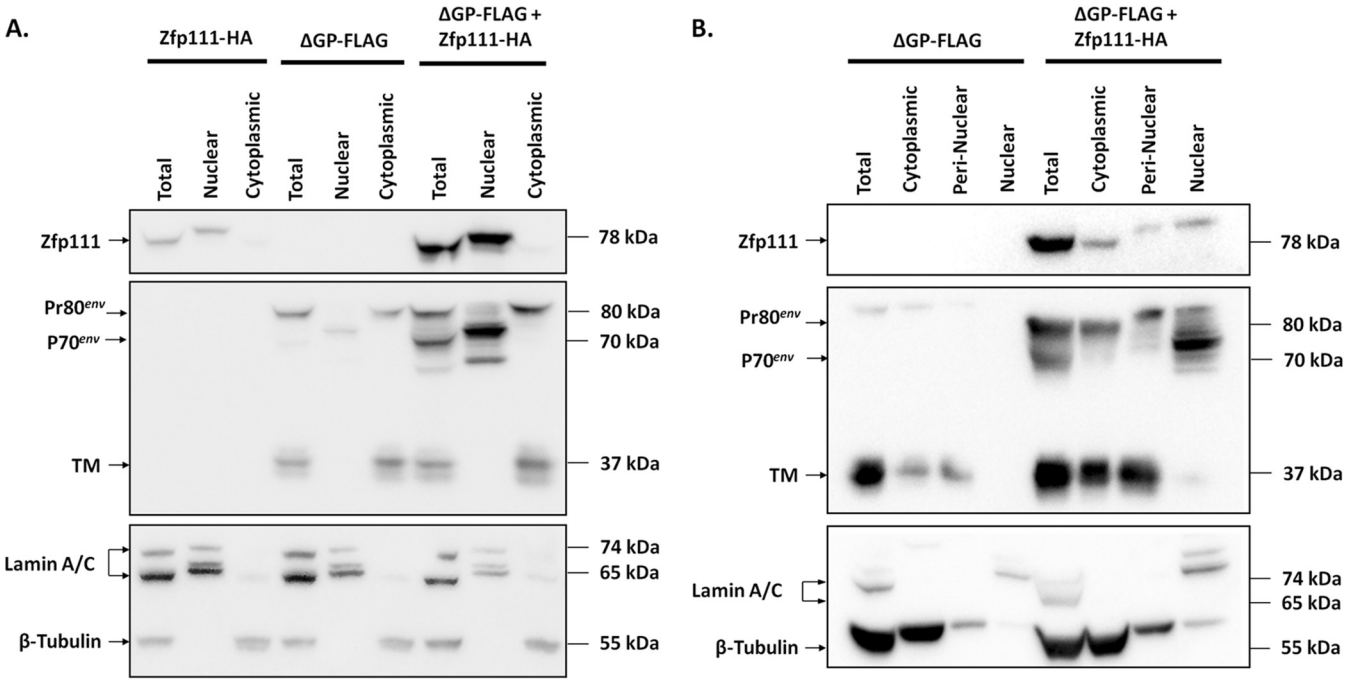

FIG 6 P70^{env} is found exclusively in the nuclear fraction. HEK 293T cells were transfected with ΔGP-FLAG, mouse Zfp111-HA, or both, as indicated. (A) Transfected cells were fractionated into nuclear and cytoplasmic fractions, as described in Materials and Methods. Total cell lysates (Total) without fractionation were also collected. Fractions were analyzed by SDS-PAGE and Western blotting, and the blot was probed and reprobed with either anti-HA (top), anti-FLAG (middle), or lamin A/C plus β-tubulin antibodies (bottom). Names and molecular masses of the observed proteins are indicated on the sides of the blot. (B) P70^{env} is not found in the perinuclear fraction. Transfected cells were subjected to further cell fractionation, generating cytoplasmic, perinuclear, and nuclear fractions. Total cell lysates without fractionation were also collected. The cell fractions were analyzed by Western blotting with anti-HA, anti-FLAG, and lamin A/C plus β-tubulin antibodies, as described above for panel A. Names and molecular masses of the observed proteins are indicated on the sides of the blot. Note that in these experiments, the mobilities of all proteins (including nuclear lamins) were slightly retarded in the nuclear samples, perhaps due to the higher-salt conditions used for preparation of the nuclear extracts.

P70^{env} was not detected in the cytoplasmic fraction at all, indicating that it is found exclusively in the nucleus.

JSRV Env, like other envelope proteins, is generally considered a cytoplasmic (plasma membrane) protein; this localization is necessary for its incorporation into the viral envelope as particles bud from the cell. Thus, it was somewhat surprising to find P70^{env} in the nuclear fraction. One possible explanation was that P70^{env} is found in the perinuclear region of the cytoplasm, which still may allow for interactions between nuclear Zfp111 and P70^{env}. A second cell fractionation procedure included washing of the nuclei with an ionic/nonionic detergent mixture, to give a perinuclear fraction separate from the rest of the cytoplasm (36, 37). Western blot analysis revealed that P70^{env} was found exclusively in the nuclear fraction along with Zfp111 and not in the perinuclear fraction (Fig. 6B). Low levels of Zfp111 were observed in the cytoplasmic and perinuclear fractions, but this likely did not reflect a relocalization of Zfp111 to the cytoplasm by JSRV Env, since the coimmunoprecipitations shown in Fig. 1 indicated that Zfp111 binds P70^{env} (which is in the nucleus) and not Pr80^{env} (which is cytoplasmic).

It was noteworthy that only the cells transfected with both ΔGP-FLAG and Zfp111-HA showed readily detectable P70^{env}. (In some but not all experiments, low levels of P70^{env} along with high levels of Pr80^{env} were detected in cells transfected with ΔGP-FLAG alone [Fig. 6A].) At the same time, in cells transfected with Zfp111 only, the Zfp111 signal was much weaker than the signal in ΔGP-FLAG- and Zfp111-cotransfected cells (Fig. 6A). This suggested that JSRV Env-HA (P70^{env}) binding in cotransfected cells may result in stabilization.

Pr80^{env} and P70^{env} differ in glycosylation levels. We next investigated the molecular basis for the differences between Pr80^{env} and P70^{env}. Like many plasma membrane proteins, JSRV Env is modified by glycosylation (23, 38, 39). The size difference between Pr80^{env} and P70^{env} could be due to differences in their glycosylation levels, the polypeptide backbones, or both. To characterize the difference between Pr80^{env} and P70^{env}, both proteins were deglycosylated by *in vitro* endoglycosidase F (Endo F) digestion, which removes all N-linked glycosylation from asparagines, the predominant glycosylation in retroviral Env proteins (40). HEK 293T cells were cotransfected with ΔGP-FLAG and Zfp111-HA and fractionated into cytoplasmic and nuclear fractions. The cytoplasmic fraction contained exclusively Pr80^{env}, while nuclei contained P70^{env}, as described above. Cytoplasmic and nuclear samples (as well as the total cell extract) were incubated with and without Endo F and then analyzed by SDS-PAGE and Western blotting for the FLAG epitope (Fig. 7). Endo F digestion of Pr80^{env} (total or cytoplasmic fractions) resulted in its conversion to a protein of 60 kDa, which represented the deglycosylated polypeptide core of Pr80^{env}. Endo F digestion of P70^{env} resulted in a comparable band of 60 kDa (nuclear fraction) (Fig. 7). This result indicated that Pr80^{env} and P70^{env} share the same polypeptide backbone but differ in their glycosylation levels.

To determine the differences in glycosylation between Pr80^{env} and P70^{env}, we first characterized the regions of Pr80^{env} that were

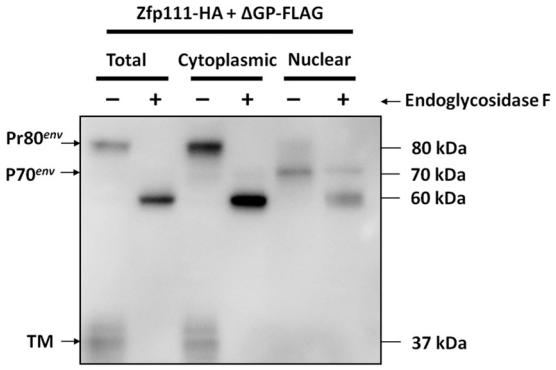

FIG 7 Deglycosylation of Pr80^{env} and P70^{env}. Total, cytoplasmic, and nuclear fractions from HEK 293T cells cotransfected with 5 μg mouse Zfp111-HA and 5 μg ΔGP-FLAG were treated with endoglycosidase F to remove N-linked glycosylation. The treated and untreated fractions were analyzed by Western blotting and probed with anti-FLAG. Names and molecular masses of the observed proteins are indicated on the sides of the blot.

glycosylated. This was accomplished by partial proteolytic cleavage with chymotrypsin combined with deglycosylation by Endo F, followed by size analysis by SDS-PAGE and Western blotting. Zfp111-HA and ΔGP-FLAG were cotransfected into HEK 293T cells, and a portion of the cytoplasmic extracts (which contained Pr80^{env} as well as cleaved SU and TM) was partially digested with limiting amounts of chymotrypsin. Some extracts were first treated with Endo F to deglycosylate the proteins and then digested with chymotrypsin. The digests were then analyzed by SDS-PAGE and Western blotting with anti-FLAG antibody. Results of a typical analysis are shown in Fig. 8A. A series of partial proteolytic products of Pr80^{env} (partial proteolytic product 1 [P1], P2, and P3) was evident in the samples treated with chymotrypsin only as well as the cleaved TM protein. Since the FLAG epitope was located at the C terminus of Pr80^{env}, only cleavage products containing the C terminus were visualized. As a result, the locations of the chymotryptic cleavage sites along Pr80^{env} could be calculated from the sizes of the products in the chymotrypsin digests. As also shown in Fig. 8A, a corresponding ladder of partial chymotryptic cleavage products (*) was observed for the samples treated with Endo F first. Comparison of sizes of the cleavage products before and after Endo F treatment could be used to calculate the amount of carbohydrate on each product. Moreover, comparison of the amounts of carbohydrate on successively smaller partial chymotrypic products could be used to infer the amount of glycosylation within regions between two chymotryptic cleavage sites. A similar analysis with a higher-percentage SDS-PAGE gel (12.5% acryl-

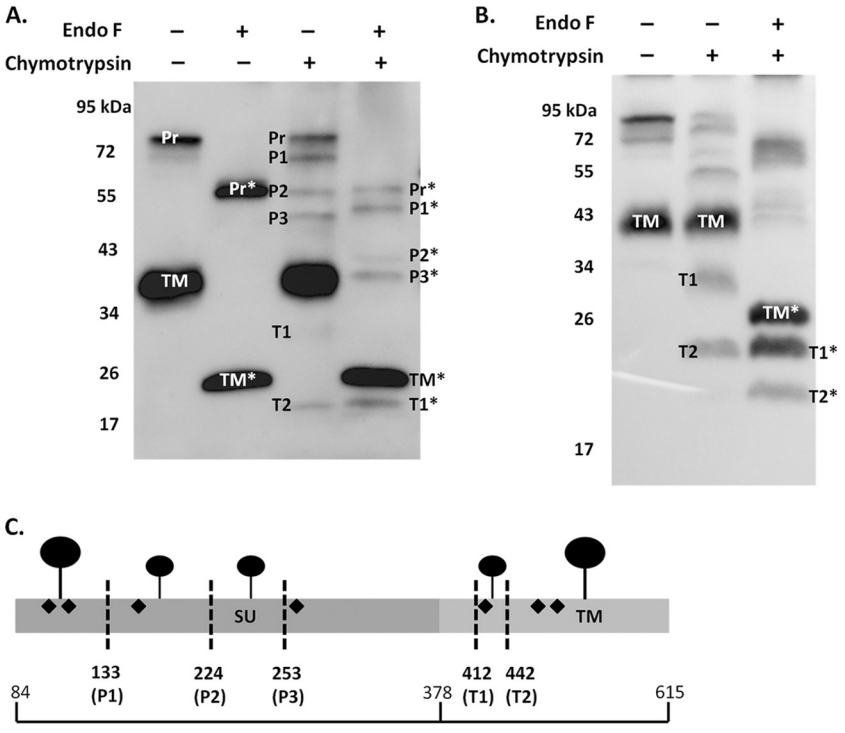

FIG 8 Characterization of glycosylation on Pr80^{env}. (A) Representative Western blot of the cytoplasmic fraction from HEK 293T cells cotransfected with ΔGP-FLAG and mouse Zfp111-HA. The sample was treated with Endo F and/or chymotrypsin as indicated, followed by SDS-PAGE and Western blotting for FLAG. The partial chymotryptic fragments are indicated as P1, P2, P3, T1, and T2 in the third lane from the left, with the corresponding fragments after Endo F treatment being marked with asterisks in the far right lane. The two left lanes show the molecular masses of the Pr80^{env} (Pr) and cleaved TM protein before and after (Pr* and TM*) Endo F treatment. The results from this and other similar experiments were used to estimate the molecular masses of the fragments, as shown in Table 3. (B) A total cell lysate from HEK 293T cells cotransfected with ΔGP-FLAG and Zfp111-HA was similarly treated with Endo F and/or chymotrypsin, with the samples being resolved in a higher-percentage acrylamide gel (12.5%) for visualization of smaller chymotryptic fragments from TM. (C) Diagram of Pr80^{env} glycosylation, with Env being divided into SU and TM regions. Residue numbering begins with the first amino acid of the Env signal peptide; the amino terminus of Pr80^{env} is located at residue 84. Estimated chymotrypsin cleavage sites are indicated by dotted black lines along with their residue location and the cleavage fragment that they result in. Predicted glycosylation sites are shown as black diamonds. Glycosylations are shown by solid circles, with the sizes being proportional to the amount of glycosylation between the two adjoining chymotryptic cleavage sites, as shown in Table 4.

TABLE 3 Glycosylation on Pr80^{env} [a]

Fragment	Mean molecular mass of Pr80^{env} (cytoplasmic) product (kDa) ± SD		Mean estimated glycosylation level (kDa) ± SD
	+ Chymo	+ Chymo + Endo F	
Pr	82 ± 4	58 ± 2	24 ± 3
P1	69 ± 3	52 ± 2	17 ± 1
P2	56 ± 2	42 ± 1	14 ± 1
P3	50 ± 2	39 ± 1	10 ± 0
TM	37 ± 3	26 ± 2	12 ± 3
T1	31 ± 0	22 ± 5	9 ± 0
T2	26 ± 9	21 ± 0	6 ± 0

[a] HEK 293T cells cotransfected with ΔGP-FLAG and Zfp111 were lysed, and portions of the cell lysate fraction containing Pr80^{env} (cytoplasm) were treated with chymotrypsin (Chymo) only or chymotrypsin with Endo F, as described in Materials and Methods, and analyzed by SDS-PAGE and Western blotting for FLAG, as shown in Fig. 8A and B. Glycosylation levels for each partial chymotryptic fragment were calculated by measuring the size difference between the glycosylated fragment (chymotrypsin only, e.g., P1) and its respective deglycosylated counterpart (chymotrypsin plus Endo F, e.g., P1*). The values shown are the mean molecular masses and standard deviations from at least 2 independent experiments. All values were rounded to the nearest whole number and are given in kilodaltons. Pr, full-length polypeptide; T1, transmembrane fragment 1.

amide) was conducted (Fig. 8B) for the smaller fragments resulting from digestion of the TM protein. Table 3 shows results of the size analysis of the partial chymotrypic cleavage products (with and without Endo F treatment) for Pr80^{env}. Overall, there was an average of 24 kDa of glycosylation on Pr80^{env} based on the size difference between glycosylated and deglycosylated Pr80^{env}. Each subsequent fragment showed a decrease in glycosylation levels. Predicted N-linked glycosylation sites and the major chymotryptic cleavage sites are indicated in Fig. 8C. The estimated glycosylation levels between each chymotryptic cleavage site of Pr80^{env} are also shown in Fig. 8C, and the amount of glycosylation between each chymotryptic site is shown in Table 4. Comparisons of the sizes of the partial chymotryptic products with and without Endo F indicated that there were glycosylation sites in the SU region of Pr80^{env} between residues 84 and 133, 134 and 224, and 225 and 253 (Fig. 8C). The amount of glycosylation between residues 84 and 133 was estimated to be ~7 kDa, that between residues 134 and 224 was ~3 kDa, and that between residues 225 and 253 was ~3 kDa (Table 4). Between residues 225 and 253, there were no predicted glycosylation sites (N-X-S/T, where X is any amino acid [41]), although there is an asparagine at residue 248 (N248). For the TM protein, there was an estimated ~12 kDa of total glycosylation. Analysis of the chymotryptic fragments from TM (T1/T1* and T2/T2*) indicated that there were ~3 kDa between residues 413 and 422 and ~6 kDa between residues 443 and 615. In principle, this could indicate ~3 kDa of glycosylation between the amino terminus of TM and residue 413, but there are no asparagines in this region. It seems most likely that all of the TM glycosylation sites are downstream of residue 413; the difference in 12 versus 9 kDa of glycosylation (calculated for TM/TM* versus T1/T1*) is within the limits of error for this analysis. In any event, this analysis indicated that glycosylation in Pr80^{env} is distributed across both the SU and TM regions.

TABLE 4 Glycosylation between chymotryptic cleavage sites in Pr80^{env} [a]

Location of cleavage site (residues) (location of larger fragment)	Estimated amt of glycosylation of Pr80^{env} (kDa)
84–133 (Pr–P1)	7
134–224 (P1–P2)	3
225–253 (P2–P3)	3
378–412 (TM–T1)	3
413–442 (T1–T2)	3
443–615 (T2–end)	6

[a] The locations of each partial chymotryptic cleavage site were calculated from the lengths of the FLAG-tagged fragment shown in Fig. 8A and B as well as examination of the Env sequence for predicted chymotryptic sites. This was possible because the FLAG tag was located at the C terminus of all detected fragments. Thus, Pr80^{env} could be divided into different regions delineated by the cleavage sites. The residues are numbered from the beginning of the Env reading frame; after cleavage of the signal peptide, the amino terminus of Pr80^{env} is located at residue 84. The amount of glycosylation between chymotryptic cleavage sites was estimated by subtracting the glycosylation levels (Table 3) of the smaller fragment from the immediately larger fragment, shown here in parentheses next to the residue ranges. All values are rounded to the nearest whole number and are shown in kilodaltons (see Fig. 8C for a graphical representation of the results).

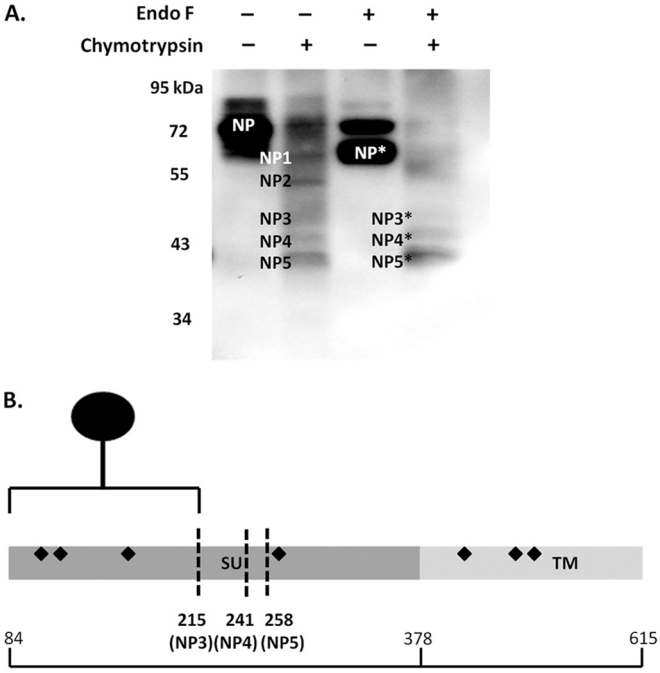

FIG 9 Glycosylation on P70^{env}. (A) Representative Western blot of the nuclear fraction from HEK 293T cells cotransfected with ΔGP-FLAG and mouse Zfp111-HA. The fraction was treated with Endo F and/or chymotrypsin and analyzed as described in the legend of Fig. 8A, with the fragments after Endo F treatment having an asterisk next to their names. The nuclear fraction was highly enriched for P70^{env} (NP) (left lane), although a small amount of Pr80^{env} was also present. Five partial chymotrypic products, NP1 to NP5, were consistently observed. Some glycosylated P70^{env} remained after Endo F digestion. The deglycosylated forms of NP1 and NP2 consistently were not resolved, but NP3 to NP5 were (fourth lane). The calculated molecular masses of the chymotryptic fragments from two independent treatments are shown in Table 5. (B) Diagram of P70^{env} glycosylation analogous to that described in the legend of Fig. 8B for Pr80^{env}. The calculated levels of glycosylation for different regions of P70^{env} are shown in Table 6.

The identification of glycosylation sites and determination of levels of P70^{env} were conducted similarly and are shown in Fig. 9 and Table 5. P70^{env} was found to have 5 partial chymotryptic cleavage sites, NP1 to NP5, based on the digestion of P70^{env} (Fig. 9A). However, the NP1 and NP2 fragments were not readily resolved by SDS-PAGE after P70^{env} had undergone deglycosylation and chymotrypsin digestion. On the other hand, NP3 to NP5

TABLE 5 Glycosylation on P70^{env} [a]

Fragment	Mean molecular mass of P70^{env} (nuclear) product (kDa) ± SD		Mean estimated glycosylation level (kDa) ± SD
	+ Chymo	+ Chymo + Endo F	
NP	72	62	10
NP1	62	Not detected	Undetermined
NP2	55	Not detected	Undetermined
NP3	50	50	0
NP4	46	46	0
NP5	41	41	0

[a] HEK 293T cells cotransfected with ΔGP-FLAG and Zfp111 were lysed, and the nuclear fraction of the cell lysate fraction containing P70^{env} (nuclear) was digested with chymotrypsin (Chymo) only or chymotrypsin plus Endo F, analogous to the analysis of Pr80^{env} (Tables 2 and 3 and Fig. 9A). Glycosylation levels for each fragment were calculated by measuring the difference in the size the glycosylated fragments and the size of their respective deglycosylated counterparts. The numbers shown are the mean molecular masses from two independent treatments. All values were rounded to the nearest whole number and are given in kilodaltons. NP, full-length polypeptide; NP1, polypeptide fragment 1.

could be resolved and were found to be the same size before and after Endo F treatment, suggesting that in the region from the cleavage site giving rise to NP3 (residue 215) to the C terminus of P70^{env}, there was no glycosylation. Based on Endo F treatment, P70^{env} had a total of 10 kDa of glycosylation that was apparently located between residues 84 and 215 (Table 6 and Fig. 9B). Compared with Pr80^{env}, P70^{env} appears to be glycosylated only at the N terminus of the polypeptide, while Pr80^{env} has glycosylation spread across the protein. It should also be noted that nuclear fractions reproducibly showed no TM protein. This indicated that P70^{env} is not cleaved into TM (or its unglycosylated version), which would be consistent with the exit of P70^{env} from the endoplasmic reticulum (ER) prior to transport into a compartment containing furin protease.

DISCUSSION

In this study, we sought to identify cellular proteins involved in transformation by JSRV Env. Through yeast 2-hybrid screening, we identified candidate proteins that interact with either the JSRV Env cytoplasmic tail or the whole Env protein, and Zfp111 was studied here. Pulldown experiments confirmed that Zfp111 interacts with JSRV Env in cells, and knockdown of *zfp111* resulted in a reduced efficiency of JSRV transformation in rat 208F cells. Conversely, overexpression of *zfp111* enhanced JSRV Env transformation. The role of Zfp111 appeared to be specific for JSRV Env transformation, since transformation by the v-*mos* oncogene was not affected by alterations in Zfp111 levels. While knockdown of *zfp111* did not affect the growth rate of normal 208F cells, knockdown in JSRV Env-transformed cells resulted in a reduction of the growth rate, suggesting that JSRV Env-transformed cells have become dependent on Zfp111 for growth. In addition, a faster-migrating form of JSRV Env was found in the nucleus, particularly when Zfp111 was coexpressed in cells. This nuclear form of Env, P70^{env}, shared the same polypeptide backbone as the standard cytoplasmic Env polyprotein precursor Pr80^{env} but differed in the extent of glycosylation. The regions of glycosylation for both Pr80^{env} and P70^{env} were mapped. In fact, it was P70^{env} that coimmunoprecipitated with Zfp111, and the interaction appeared to stabilize both proteins.

Zfp111, also known as rKr2, was originally identified as a Cys2/His2 zinc finger protein with 19 zinc fingers in the C-terminal domain (42). It is a member of the Krüppel family of zinc finger proteins, characterized by the presence of a Krüppel-associated box (KRAB) (43). Like other KRAB-containing zinc finger proteins, Zfp111 contains an amino-terminal KRAB domain that for other KRAB proteins confers transcriptional repression activity (43). In adult rats, Zfp111 is localized in the nucleus in oligodendrocytes (42), and *zfp111* RNA is expressed at the highest levels in oligodendrocytes of the cerebellum/spinal cord and in testis, but it is also found at lower levels in liver, spleen, and lungs (35, 42). Target genes for Zfp111 have not been identified, although it has been suggested that it plays a role in oligodendrocyte differentiation from neuronal stem cells (42). In general, Krüppel family zinc finger proteins have roles in cell differentiation, proliferation, and tumorigenesis (44).

Several lines of evidence supported a role for Zfp111 in JSRV Env transformation. First, knockdown of endogenous *zfp111* expression by transduction with a lentiviral shRNA vector significantly reduced JSRV Env transformation in rat 208F cells. Moreover, cotransfection of a shRNA-resistant *zfp111* expression plasmid partially restored JSRV Env transformation in *zfp111* knockdown cells (Fig. 3). While statistically significant, the reduction in transformation in Zfp111 knockdown cells was modest (ca. 50%), which was correlated with the partial *zfp111* knockdown by the most efficient lentiviral plasmid available, r36-2 (ca. 50 to 65%). Many viral oncogenes transform cells by interacting with multiple cellular proteins, and interruption of individual interactions could reduce transformation without abolishing it (45–47). Second, overexpression of *zfp111* enhanced JSRV Env transformation. Third, while knockdown of *zfp111* did not affect the growth rate of parental rat 208F cells, knockdown in JSRV-transformed cells reduced the growth rate. This indicated that JSRV-transformed cells became dependent on Zfp111. Moreover, the role of Zfp111 in transformation was specific for JSRV Env, since transformation by the viral oncogene v-*mos* (which does not activate signaling through PI3K-Akt and Ras-Raf-MEK [29, 31, 48, 49]) was not affected by either the knockdown or overexpression of Zfp111. The fact that v-*mos* transformation was not affected in cells transduced with the r36-2 knockdown vector also indicated that the reduction in JSRV Env transformation was not due to general or off-target effects.

When Zfp111 was first identified as a candidate interactor with JSRV Env, a role in transformation was challenging to conceive, since Zfp111 is a nuclear protein and Env was considered to be cytoplasmic. The findings of the stabilization of Zfp111 by Env binding and of the appearance of nuclear Env after Zfp111 binding raise several possible mechanisms. First, Zfp111 could chaperone Env to the nucleus, where Env could cause transformation

TABLE 6 Estimated glycosylation between chymotryptic cleavage sites in P70^{env} [a]

Location of fragment (residues) (location of larger fragment)	Amt of glycosylation of P70^{env} (kDa)
84–215 (NP–NP3)	10
216–241 (NP3–NP4)	0
242–258 (NP4–NP5)	0
259–615 (NP5–end)	0

[a] The results from Table 5 and Fig. 9A were analyzed as for Table 4 to determine the location of glycosylation on P70^{env}. The results are shown in Fig. 9B.

in conjunction with other proteins. Second, nuclear Env could modify the activity of Zfp111 so that the latter protein induces transformation. A third possibility is that cytoplasmic Env relocalizes a portion of Zfp111 to the cytoplasm, where it is involved in transformation; however, we have not detected cytoplasmic relocalization of Zfp111 by either immunofluorescence or cell fractionation (T. Hsu and H. Fan, unpublished data). It should be noted that overexpression of Zfp111 in the absence of JSRV Env does not result in transformation (Fig. 4), so JSRV is not transforming cells simply by enhancing levels of Zfp111.

One question is how P70^{env} enters the nucleus while Pr80^{env} does not. The facts that both of these proteins are glycosylated and that they share polypeptide backbones indicate that they both are initially translocated into the ER during translation. One possibility is that a portion of the Env polyprotein destined to become P70^{env} associates with a cellular protein(s) that directs it to the nucleus. Zfp111 would be a prime candidate for such a protein since it binds and appears to stabilize P70^{env} in cotransfections, and it is a nuclear protein. However, it is currently unclear if or how Zfp111 can enter the ER, which would be required for it to conduct P70^{env} to the nucleus; nevertheless, the coimmunoprecipitation and stabilization experiments clearly indicate that these two proteins interact in some compartment within the cell. Alternatively, it is possible that some other cellular protein directs P70^{env} to the nucleus, where the observed binding with Zfp111 (and stabilization) takes place. Another possibility could be that the Env polyprotein contains a nuclear localization signal (NLS) that directs a portion of it to the nucleus (P70^{env}), with the remainder continuing through the ER to the plasma membrane (Pr80^{env}). It is noteworthy that the JSRV Env coding sequences also specify a regulatory protein, Rej, in the signal peptide (50–52). Rej regulates unspliced viral RNA translation and nuclear export, analogous to the murine mammary tumor virus (MMTV) Rem protein and the HIV-1 Rev protein (53–56). Indeed, Rej carries a NLS; however, as a signal peptide, it is cleaved from the Env polyprotein precursor during translation, so its NLS is not likely to be present in P70^{env} or Pr80^{env}. While scanning of the P70^{env} protein sequence did not reveal an obvious NLS (T. Hsu, unpublished data), it is possible that there is a cryptic NLS. Perhaps differential (lower) glycosylation of P70^{env} exposes a cryptic NLS in those molecules destined for nuclear import, while it is shielded in fully glycosylated Pr80^{env}, which is transported to the plasma membrane for incorporation into viral envelopes. A related question is how P70^{env} gains access from the ER (where it is glycosylated) to the cytosol, from where it is presumably imported into the nucleus. In the case of the MMTV Rem protein, the ER-associated protein degradation (ERAD) pathway is responsible for retrotranslocation of this protein (the signal peptide of the MMTV Env polyprotein) from the ER back to the cytosol (57). The normal function of ERAD is to transport misfolded proteins (marked by ubiquitination) from the ER back to the cytosol for proteosomal degradation; it seems possible that, like MMTV Rem, JSRV P70^{env} could be transported back to the cytoplasm by this mechanism without degradation. In mammalian cells, misfolded proteins are targeted to the ERAD pathway following the removal of 3 to 4 mannose residues by ER processing alpha 1,2-mannosidase (ER ManI) (58–61). P70^{env} could be a misfolded version of Env (or at least appears to be misfolded to the ERAD machinery) that becomes more abundant in cells that are cotransfected with Zfp111. After partial mannose removal, misfolded Env (P70^{env}) would enter the ERAD pathway to escape to the cytoplasm, where it would be transported back into the nucleus by a yet-to-be-identified chaperone protein.

Future experiments will be needed to map the exact locations of the glycosylation sites on Pr80^{env} and P70^{env} as well as to characterize glycosylation on these two proteins. To identify sites of glycosylation, mutations in putative glycosylation sites could be generated and evaluated for glycosylation levels in both Pr80^{env} and P70^{env}. An early attempt has been made to verify the putative glycosylation sites on JSRV Env via site-directed mutagenesis (Hsu, unpublished). Ultimately, other techniques such as mass spectrometry in conjunction with digestions with proteases and glycosidases could be used to further characterize the nature of glycosylation on Pr80^{env} and P70^{env}, but they are beyond the scope of this study.

As a cytoplasmic protein, JSRV Env was previously thought to induce cell transformation by the activation of growth signaling pathways in the cytoplasm. The identification of nuclear Zfp111 as a JSRV Env-interacting protein that is important for JSRV transformation was unexpected, and the additional finding of a nuclear version of JSRV Env was even more surprising. The identification of nuclear P70^{env} and its interaction with nuclear Zfp111 in transformation indicates that the mechanism of JSRV Env transformation may extend beyond cytoplasmic signaling pathways and into the nucleus. One model could be that P70^{env} sequesters Zfp111 into an inactive complex, relieving its putative transcriptional repression. However, this would not be consistent with the fact that overexpression of Zfp111 enhances JSRV transformation. This rather might suggest that P70^{env} converts Zfp111 from a repressive protein to one that activates transcription or some other function contributing to cell transformation.

The transformation experiments conducted in this study were performed on rat 208F fibroblasts. This was done because the yeast 2-hybrid screen identified mouse *zfp111* as the interacting protein, and mouse and rat *zfp111* are highly related. Rat 208F cells are a robust system for transformation, with very low (no) background. Ultimately, it would be desirable to investigate if this interaction is important for tumorigenesis in the natural target of JSRV, ovine lung epithelial cells. To accomplish this, the ovine orthologue of *zfp111* must be identified, and a quantitative system for transformation of ovine lung epithelial cells must be developed. As an intermediate step, it will be important to determine if the ovine *zfp111* orthologue is expressed in lung epithelial cells.

Shortly before this work was submitted, a related study was accepted for publication in this journal. Monot et al. (62) also used a yeast 2-hybrid screen and identified a different JSRV Env-interacting protein, Ral binding protein (RalBP1). They also showed that RalBP1 interacts with JSRV Env in cells and that it is important for transformation by modulating signaling through mTOR/p70S6K. It would seem to be acting independently of the Env-Zfp111 interaction described here. Thus, as mentioned above, JSRV Env likely causes transformation through interactions with multiple cellular proteins.

ACKNOWLEDGMENTS

This work was supported by grants R01CA94188 and P30CA062203 from the National Cancer Institute. T.H. was partially supported by NIH training grant 5-T32-AI 07319.

We thank Takayuki Nitta, Andy Hofacre, and Chassidy Johnson for helpful suggestions and Parvez Malak for help with some of the assays

performed in this study. We acknowledge support from the Optical Biology shared resource of the UCI Chao Family Comprehensive Cancer Center and the UCI Cancer Research Institute.

REFERENCES

1. **Palmarini M, Fan H.** 2001. Retrovirus-induced ovine pulmonary adenocarcinoma, an animal model for lung cancer. J Natl Cancer Inst **93:**1603–1614. http://dx.doi.org/10.1093/jnci/93.21.1603.
2. **Palmarini M, Sharp JM, de las Heras M, Fan H.** 1999. Jaagsiekte sheep retrovirus is necessary and sufficient to induce a contagious lung cancer in sheep. J Virol **73:**6964–6972.
3. **Travis WD, Brambilla E, Noguchi M, Nicholson AG, Geisinger KR, Yatabe Y, Beer DG, Powell CA, Riely GJ, Van Schil PE, Garg K, Austin JH, Asamura H, Rusch VW, Hirsch FR, Scagliotti G, Mitsudomi T, Huber RM, Ishikawa Y, Jett J, Sanchez-Cespedes M, Sculier JP, Takahashi T, Tsuboi M, Vansteenkiste J, Wistuba I, Yang PC, Aberle D, Brambilla C, Flieder D, Franklin W, Gazdar A, Gould M, Hasleton P, Henderson D, Johnson B, Johnson D, Kerr K, Kuriyama K, Lee JS, Miller VA, Petersen I, Roggli V, Rosell R, Saijo N, Thunnissen E, Tsao M, Yankelewitz D.** 2011. International Association for the Study of Lung Cancer/American Thoracic Society/European Respiratory Society international multidisciplinary classification of lung adenocarcinoma. J Thorac Oncol **6:**244–285. http://dx.doi.org/10.1097/JTO.0b013e318206a221.
4. **Palmarini M, Fan H, Sharp JM.** 1997. Sheep pulmonary adenomatosis: a unique model of retrovirus-associated lung cancer. Trends Microbiol **5:**478–483. http://dx.doi.org/10.1016/S0966-842X(97)01162-1.
5. **Mornex JF, Thivolet F, De las Heras M, Leroux C.** 2003. Pathology of human bronchioloalveolar carcinoma and its relationship to the ovine disease. Curr Top Microbiol Immunol **275:**225–248.
6. **Youssef G, Wallace WA, Dagleish MP, Cousens C, Griffiths DJ.** 2015. Ovine pulmonary adenocarcinoma: a large animal model for human lung cancer. ILAR J **56:**99–115. http://dx.doi.org/10.1093/ilar/ilv014.
7. **York DF, Vigne R, Verwoerd DW, Querat G.** 1992. Nucleotide sequence of the Jaagsiekte retrovirus, an exogenous and endogenous type D and B retrovirus of sheep and goats. J Virol **66:**4930–4939.
8. **Verwoerd DW, Williamson AL, De Villiers EM.** 1980. Aetiology of Jaagsiekte: transmission by means of subcellular fractions and evidence for the involvement of a retrovirus. Onderstepoort J Vet Res **47:**275–280.
9. **Sharp JM, Angus KW, Gray EW, Scott FM.** 1983. Rapid transmission of sheep pulmonary adenomatosis (Jaagsiekte) in young lambs. Brief report. Arch Virol **78:**89–95. http://dx.doi.org/10.1007/BF01310861.
10. **Maeda N, Palmarini M, Murgia C, Fan H.** 2001. Direct transformation of rodent fibroblasts by Jaagsiekte sheep retrovirus DNA. Proc Natl Acad Sci U S A **98:**4449–4454. http://dx.doi.org/10.1073/pnas.071547598.
11. **Rai SK, Duh FM, Vigdorovich V, Danilkovitch-Miagkova A, Lerman MI, Miller AD.** 2001. Candidate tumor suppressor HYAL2 is a glycosylphosphatidylinositol (GPI)-anchored cell-surface receptor for Jaagsiekte sheep retrovirus, the envelope protein of which mediates oncogenic transformation. Proc Natl Acad Sci U S A **98:**4443–4448. http://dx.doi.org/10.1073/pnas.071572898.
12. **Allen TE, Sherrill KJ, Crispell SM, Perrott MR, Carlson JO, DeMartini JC.** 2002. The Jaagsiekte sheep retrovirus envelope gene induces transformation of the avian fibroblast cell line DF-1 but does not require a conserved SH2 binding domain. J Gen Virol **83:**2733–2742.
13. **Liu SL, Miller AD.** 2005. Transformation of Madin-Darby canine kidney epithelial cells by sheep retrovirus envelope proteins. J Virol **79:**927–933. http://dx.doi.org/10.1128/JVI.79.2.927-933.2005.
14. **Wootton SK, Halbert CL, Miller AD.** 2005. Sheep retrovirus structural protein induces lung tumours. Nature **434:**904–907. http://dx.doi.org/10.1038/nature03492.
15. **Linnerth-Petrik NM, Santry LA, Yu DL, Wootton SK.** 2012. Adeno-associated virus vector mediated expression of an oncogenic retroviral envelope protein induces lung adenocarcinomas in immunocompetent mice. PLoS One **7:**e51400. http://dx.doi.org/10.1371/journal.pone.0051400.
16. **Caporale M, Cousens C, Centorame P, Pinoni C, De las Heras M, Palmarini M.** 2006. Expression of the Jaagsiekte sheep retrovirus envelope glycoprotein is sufficient to induce lung tumors in sheep. J Virol **80:**8030–8037. http://dx.doi.org/10.1128/JVI.00474-06.
17. **De las Heras M, Ortin A, Cousens C, Minguijon E, Sharp JM.** 2003. Enzootic nasal adenocarcinoma of sheep and goats. Curr Top Microbiol Immunol **275:**201–223.
18. **Dirks C, Duh FM, Rai SK, Lerman MI, Miller AD.** 2002. Mechanism of cell entry and transformation by enzootic nasal tumor virus. J Virol **76:**2141–2149. http://dx.doi.org/10.1128/jvi.76.5.2141-2149.2002.
19. **Alberti A, Murgia C, Liu SL, Mura M, Cousens C, Sharp M, Miller AD, Palmarini M.** 2002. Envelope-induced cell transformation by ovine betaretroviruses. J Virol **76:**5387–5394. http://dx.doi.org/10.1128/JVI.76.11.5387-5394.2002.
20. **DeMartini JC, Bishop JV, Allen TE, Jassim FA, Sharp JM, de las Heras M, Voelker DR, Carlson JO.** 2001. Jaagsiekte sheep retrovirus proviral clone JSRV(JS7), derived from the JS7 lung tumor cell line, induces ovine pulmonary carcinoma and is integrated into the surfactant protein A gene. J Virol **75:**4239–4246. http://dx.doi.org/10.1128/JVI.75.9.4239-4246.2001.
21. **Songyang Z, Shoelson SE, Chaudhuri M, Gish G, Pawson T, Haser WG, King F, Roberts T, Ratnofsky S, Lechleider Neel BG, Birge RB, Fajardo JE, Chou MM, Hanafusa H, Schaffhausen B, Cantley LC.** 1993. SH2 domains recognize specific phosphopeptide sequences. Cell **72:**767–778. http://dx.doi.org/10.1016/0092-8674(93)90404-E.
22. **Palmarini M, Maeda N, Murgia C, De-Fraja C, Hofacre A, Fan H.** 2001. A phosphatidylinositol 3-kinase docking site in the cytoplasmic tail of the Jaagsiekte sheep retrovirus transmembrane protein is essential for envelope-induced transformation of NIH 3T3 cells. J Virol **75:**11002–11009. http://dx.doi.org/10.1128/JVI.75.22.11002-11009.2001.
23. **Hofacre A, Fan H.** 2004. Multiple domains of the Jaagsiekte sheep retrovirus envelope protein are required for transformation of rodent fibroblasts. J Virol **78:**10479–10489. http://dx.doi.org/10.1128/JVI.78.19.10479-10489.2004.
24. **Liu SL, Lerman MI, Miller AD.** 2003. Putative phosphatidylinositol 3-kinase (PI3K) binding motifs in ovine betaretrovirus Env proteins are not essential for rodent fibroblast transformation and PI3K/Akt activation. J Virol **77:**7924–7935. http://dx.doi.org/10.1128/JVI.77.14.7924-7935.2003.
25. **Cousens C, Maeda N, Murgia C, Dagleish MP, Palmarini M, Fan H.** 2007. In vivo tumorigenesis by Jaagsiekte sheep retrovirus (JSRV) requires Y590 in Env TM, but not full-length orfX open reading frame. Virology **367:**413–421. http://dx.doi.org/10.1016/j.virol.2007.06.004.
26. **Liu SL, Miller AD.** 2007. Oncogenic transformation by the Jaagsiekte sheep retrovirus envelope protein. Oncogene **26:**789–801. http://dx.doi.org/10.1038/sj.onc.1209850.
27. **Zavala G, Pretto C, Chow YH, Jones L, Alberti A, Grego E, De las Heras M, Palmarini M.** 2003. Relevance of Akt phosphorylation in cell transformation induced by Jaagsiekte sheep retrovirus. Virology **312:**95–105. http://dx.doi.org/10.1016/S0042-6822(03)00205-8.
28. **Suau F, Cottin V, Archer F, Croze S, Chastang J, Cordier G, Thivolet-Bejui F, Mornex JF, Leroux C.** 2006. Telomerase activation in a model of lung adenocarcinoma. Eur Respir J **27:**1175–1182. http://dx.doi.org/10.1183/09031936.06.00125105.
29. **Maeda N, Fu W, Ortin A, de las Heras M, Fan H.** 2005. Roles of the Ras-MEK-mitogen-activated protein kinase and phosphatidylinositol 3-kinase-Akt-mTOR pathways in Jaagsiekte sheep retrovirus-induced transformation of rodent fibroblast and epithelial cell lines. J Virol **79:**4440–4450. http://dx.doi.org/10.1128/JVI.79.7.4440-4450.2005.
30. **Quade K.** 1979. Transformation of mammalian cells by avian myelocytomatosis virus and avian erythroblastosis virus. Virology **98:**461–465. http://dx.doi.org/10.1016/0042-6822(79)90569-5.
31. **Maeda N, Inoshima Y, Fruman DA, Brachmann SM, Fan H.** 2003. Transformation of mouse fibroblasts by Jaagsiekte sheep retrovirus envelope does not require phosphatidylinositol 3-kinase. J Virol **77:**9951–9959. http://dx.doi.org/10.1128/JVI.77.18.9951-9959.2003.
32. **Dhar R, McClements WL, Enquist LW, Vande Woude GF.** 1980. Nucleotide sequences of integrated Moloney sarcoma provirus long terminal repeats and their host and viral junctions. Proc Natl Acad Sci U S A **77:**3937–3941. http://dx.doi.org/10.1073/pnas.77.7.3937.
33. **Gyuris J, Golemis E, Chertkov H, Brent R.** 1993. Cdi1, a human G1 and S phase protein phosphatase that associates with Cdk2. Cell **75:**791–803. http://dx.doi.org/10.1016/0092-8674(93)90498-F.
34. **Wiznerowicz M, Trono D.** 2003. Conditional suppression of cellular genes: lentivirus vector-mediated drug-inducible RNA interference. J Virol **77:**8957–8961. http://dx.doi.org/10.1128/JVI.77.16.8957-8951.2003.
35. **Pott U, Thiesen HJ, Colello RJ, Schwab ME.** 1995. A new Cys2/His2 zinc finger gene, rKr2, is expressed in differentiated rat oligodendrocytes and encodes a protein with a functional repressor domain. J Neurochem **65:**1955–1966.
36. **Penman S.** 1966. RNA metabolism in the HeLa cell nucleus. J Mol Biol **17:**117–130. http://dx.doi.org/10.1016/S0022-2836(66)80098-0.
37. **Galvis AE, Fisher HE, Nitta T, Fan H, Camerini D.** 2014. Impairment of

HIV-1 cDNA synthesis by DBR1 knockdown. J Virol **88:**7054–7069. http://dx.doi.org/10.1128/JVI.00704-14.
38. **Cote M, Kucharski TJ, Liu SL.** 2008. Enzootic nasal tumor virus envelope requires a very acidic pH for fusion activation and infection. J Virol **82:**9023–9034. http://dx.doi.org/10.1128/JVI.00648-08.
39. **Hull S, Lim J, Hamil A, Nitta T, Fan H.** 2012. Analysis of Jaagsiekte sheep retrovirus (JSRV) envelope protein domains in transformation. Virus Genes **45:**508–517. http://dx.doi.org/10.1007/s11262-012-0793-y.
40. **Petropoulos C.** 1997. Retroviral taxonomy, protein structures, sequences, and genetic maps, p 757–805. *In* Coffin JM, Hughes SH, Varmus HE (ed), Retroviruses. Cold Spring Harbor Laboratory Press, Cold Spring Harbor, NY.
41. **Medzihradszky KF.** 2005. Characterization of protein N-glycosylation. Methods Enzymol **405:**116–138. http://dx.doi.org/10.1016/S0076-6879(05)05006-8.
42. **Lovas G, Li W, Pott U, Verga T, Hudson LD.** 2001. Expression of the Kruppel-type zinc finger protein rKr2 in the developing nervous system. Glia **34:**110–120. http://dx.doi.org/10.1002/glia.1046.
43. **Urrutia R.** 2003. KRAB-containing zinc-finger repressor proteins. Genome Biol **4:**231. http://dx.doi.org/10.1186/gb-2003-4-10-231.
44. **Bieker JJ.** 2001. Kruppel-like factors: three fingers in many pies. J Biol Chem **276:**34355–34358. http://dx.doi.org/10.1074/jbc.R100043200.
45. **Fluck MM, Schaffhausen BS.** 2009. Lessons in signaling and tumorigenesis from polyomavirus middle T antigen. Microbiol Mol Biol Rev **73:**542–563. http://dx.doi.org/10.1128/MMBR.00009-09.
46. **Cheng AM, Saxton TM, Sakai R, Kulkarni S, Mbamalu G, Vogel W, Tortorice CG, Cardiff RD, Cross JC, Muller WJ, Pawson T.** 1998. Mammalian Grb2 regulates multiple steps in embryonic development and malignant transformation. Cell **95:**793–803. http://dx.doi.org/10.1016/S0092-8674(00)81702-X.
47. **Maroulakou IG, Oemler W, Naber SP, Tsichlis PN.** 2007. Akt1 ablation inhibits, whereas Akt2 ablation accelerates, the development of mammary adenocarcinomas in mouse mammary tumor virus (MMTV)-ErbB2/neu and MMTV-polyoma middle T transgenic mice. Cancer Res **67:**167–177. http://dx.doi.org/10.1158/0008-5472.CAN-06-3782.
48. **Nebreda AR, Hill C, Gomez N, Cohen P, Hunt T.** 1993. The protein kinase mos activates MAP kinase kinase in vitro and stimulates the MAP kinase pathway in mammalian somatic cells in vivo. FEBS Lett **333:**183–187. http://dx.doi.org/10.1016/0014-5793(93)80401-F.
49. **Posada J, Yew N, Ahn NG, Vande Woude GF, Cooper JA.** 1993. Mos stimulates MAP kinase in Xenopus oocytes and activates a MAP kinase kinase in vitro. Mol Cell Biol **13:**2546–2553.
50. **Nitta T, Hofacre A, Hull S, Fan H.** 2009. Identification and mutational analysis of a Rej response element in Jaagsiekte sheep retrovirus RNA. J Virol **83:**12499–12511. http://dx.doi.org/10.1128/JVI.01754-08.
51. **Hofacre A, Nitta T, Fan H.** 2009. Jaagsiekte sheep retrovirus encodes a regulatory factor, Rej, required for synthesis of Gag protein. J Virol **83:**12483–12498. http://dx.doi.org/10.1128/JVI.01747-08.
52. **Caporale M, Arnaud F, Mura M, Golder M, Murgia C, Palmarini M.** 2009. The signal peptide of a simple retrovirus envelope functions as a posttranscriptional regulator of viral gene expression. J Virol **83:**4591–4604. http://dx.doi.org/10.1128/JVI.01833-08.
53. **Malim MH, Hauber J, Le SY, Maizel JV, Cullen BR.** 1989. The HIV-1 rev trans-activator acts through a structured target sequence to activate nuclear export of unspliced viral mRNA. Nature **338:**254–257. http://dx.doi.org/10.1038/338254a0.
54. **D'Agostino DM, Felber BK, Harrison JE, Pavlakis GN.** 1992. The Rev protein of human immunodeficiency virus type 1 promotes polysomal association and translation of gag/pol and vpu/env mRNAs. Mol Cell Biol **12:**1375–1386.
55. **Mertz JA, Simper MS, Lozano MM, Payne SM, Dudley JP.** 2005. Mouse mammary tumor virus encodes a self-regulatory RNA export protein and is a complex retrovirus. J Virol **79:**14737–14747. http://dx.doi.org/10.1128/JVI.79.23.14737-14747.2005.
56. **Indik S, Gunzburg WH, Salmons B, Rouault F.** 2005. A novel, mouse mammary tumor virus encoded protein with Rev-like properties. Virology **337:**1–6. http://dx.doi.org/10.1016/j.virol.2005.03.040.
57. **Byun H, Halani N, Mertz JA, Ali AF, Lozano MM, Dudley JP.** 2010. Retroviral Rem protein requires processing by signal peptidase and retrotranslocation for nuclear function. Proc Natl Acad Sci U S A **107:**12287–12292. http://dx.doi.org/10.1073/pnas.1004303107.
58. **Kitzmuller C, Caprini A, Moore SE, Frenoy JP, Schwaiger E, Kellermann O, Ivessa NE, Ermonval M.** 2003. Processing of N-linked glycans during endoplasmic-reticulum-associated degradation of a short-lived variant of ribophorin I. Biochem J **376:**687–696. http://dx.doi.org/10.1042/bj20030887.
59. **Hosokawa N, Tremblay LO, You Z, Herscovics A, Wada I, Nagata K.** 2003. Enhancement of endoplasmic reticulum (ER) degradation of misfolded null Hong Kong alpha1-antitrypsin by human ER mannosidase I. J Biol Chem **278:**26287–26294. http://dx.doi.org/10.1074/jbc.M303395200.
60. **Frenkel Z, Gregory W, Kornfeld S, Lederkremer GZ.** 2003. Endoplasmic reticulum-associated degradation of mammalian glycoproteins involves sugar chain trimming to Man6-5GlcNAc2. J Biol Chem **278:**34119–34124. http://dx.doi.org/10.1074/jbc.M305929200.
61. **Ermonval M, Kitzmuller C, Mir AM, Cacan R, Ivessa NE.** 2001. N-glycan structure of a short-lived variant of ribophorin I expressed in the MadIA214 glycosylation-defective cell line reveals the role of a mannosidase that is not ER mannosidase I in the process of glycoprotein degradation. Glycobiology **11:**565–576. http://dx.doi.org/10.1093/glycob/11.7.565.
62. **Monot M, Erny A, Gineys B, Desloire S, Dolmazon C, Aublin-Gex A, Lotteau V, Archer F, Leroux C.** 2015. Early steps of Jaagsiekte sheep retrovirus-mediated cell transformation involve the interaction between Env and the RALBP1 cellular protein. J Virol **89:**8462–8473. http://dx.doi.org/10.1128/JVI.00590-15.